The Canadian Mineralogist
Vol. 48, pp. 335-350 (2010)
DOI: 10.3749/canmin.48.2.335

METARAUCHITE, $Ni(UO_2)_2(AsO_4)_2•8H_2O$, FROM JÁCHYMOV, CZECH REPUBLIC, AND SCHNEEBERG, GERMANY: A NEW MEMBER OF THE AUTUNITE GROUP

JAKUB PLÁŠIL[§], JIŘÍ SEJKORA AND JIŘÍ ČEJKA

Department of Mineralogy and Petrology, National Museum, Václavské náměstí 68, CZ–115 79, Praha 1, Czech Republic

MILAN NOVÁK

Department of Geological Science, Faculty of Science, Masaryk University, Kotlářská 2, CZ–611 37, Brno, Czech Republic

JOAN VIÑALS

Department of Materials Science and Metallurgical Engineering, University of Barcelona, Martí i Franqués 1, E–08028, Barcelona, Spain

PETR ONDRUŠ AND FRANTIŠEK VESELOVSKÝ

Czech Geological Survey, Geologická 6, CZ–152 00, Praha 5, Czech Republic

PAVEL ŠKÁCHA, JAN JEHLIČKA AND VIKTOR GOLIÁŠ

Institute of Geochemistry, Mineralogy and Mineral Resources, Charles University in Prague, Faculty of Science, Albertov 6, CZ–128 43, Praha 2, Czech Republic

JAN HLOUŠEK

U Roháčových kasáren 24, CZ–100 00, Praha 10, Czech Republic

ABSTRACT

Metarauchite, a new mineral species of the autunite group, ideally $Ni(UO_2)_2(AsO_4)_2•8H_2O$, is triclinic, space group $P\bar{1}$, *a* 7.194(4), *b* 9.713(5), *c* 13.201(9) Å, α 75.79(3), β 83.92(5), γ 81.59(4)°, *V* 882.2(9) Å^3, *Z* = 2, D_{calc} = 3.81 g•cm^{-3}. It forms crystalline aggregates consisting of yellow to light greenish yellow, translucent to transparent tabular crystals with a vitreous luster, exceptionally up to 0.8 mm in size. They have grown on a surface of altered primary mineral phases: uraninite, arsenopyrite, and nickelskutterudite. Metarauchite is very brittle, with a perfect (011) cleavage and an uneven fracture. The Mohs hardness is about 2. The mineral is not fluorescent either in short- and long-wavelength UV radiation. Metarauchite is biaxial negative, α 1.625(3), β ≈ γ 1.649; the calculated *2V* is 52° with a β of 1.646 and a γ of 1.651, and it is 23° with a β of 1.649 and a γ of 1.650. Metarauchite is not pleochroic. Results of a chemical analysis of the holotype sample, normalized to a total of 100 wt.%, yielded: NiO 6.05, CoO 0.91, MgO 0.09, UO_3 56.72, As_2O_5 21.31, P_2O_5 0.22, SiO_2 0.09, H_2O 14.61 (from thermal analysis), with a total of 100 wt.% giving the empirical formula $(Ni_{0.82}Co_{0.12}Mg_{0.02})_{\Sigma 0.96}(UO_2)_{2.01}[(AsO_4)_{1.88}(PO_4)_{0.03}(SiO_4)_{0.02}]_{\Sigma 1.93}•8.21H_2O$ (on the basis of 20 O,OH atoms). According to the thermal analysis, metarauchite dehydrates in several steps, with a total weight loss of 14.61 wt.%, which corresponds to 8.21 H_2O. The infrared spectrum of metarauchite was studied and complemented with its Raman spectrum. Stretching and bending vibrations of the $(UO_2)^{2+}$, $(AsO_4)^{3-}$ and H_2O units were tentatively assigned. Furthermore, U–O bond lengths in uranyl and O–H...O hydrogen-bond lengths were inferred from the spectra. Metarauchite occurs at the Schweitzer vein, in the Jáchymov (St. Joachimsthal) ore district, Czech Republic (type locality), in association with metazeunerite, erythrite and gypsum. Selected data for metarauchite from Schneeberg, Germany, associated with Ni-rich metanováčekite and metazeunerite also are given.

§ *E-mail address*: jakub_plasil@nm.cz

Key words: new mineral species, metarauchite, uranyl, X-ray powder data, electron-microprobe data, thermal analysis, infrared spectroscopy, Raman spectroscopy, uranyl-bond lengths, hydrogen-bond lengths, Jáchymov, Czech Republic, Schneeberg, Germany.

Sommaire

Nous décrivons la métarauchite, nouvelle espèce minérale du groupe de l'autunite, de formule idéale $Ni(UO_2)_2(AsO_4)_2•8H_2O$, triclinique, groupe spatial $P\bar{1}$, *a* 7.194(4), *b* 9.713(5), *c* 13.201(9) Å, α 75.79(3), β 83.92(5), γ 81.59(4)°, *V* 882.2(9) Å^3, *Z* = 2, D_{calc} = 3.81 g•cm^{-3}. Elle se présente en agrégats de cristaux jaunes à jaune légèrement verdâtre, translucides à transparents, tabulaires, avec un éclat vitreux, et atteignant exceptionellement une dimension de 0.8 mm. Ils recouvrent la surface de phases primaires altérées: uraninite, arsénopyrite, et nickelskutterudite. La métarauchite est très cassante, ayant un clivage (011) parfait et une fracture inégale. La dureté de Mohs est d'environ 2. Le minéral n'est pas fluorescent en lumière ultra-violette, ondes courtes ou longues. La métarauchite est biaxe négative, α 1.625(3), β ≈ γ 1.649; l'angle *2V* est 52° avec un β de 1.646 et un γ de 1.651, et il est 23° avec un β de 1.649 et un γ de 1.650. La mérauchite est non pléochroïque. Les résultats d'analyses chimiques de l'échantillon holotype, normalisés à un total de 100% (poids), ont donné: NiO 6.05, CoO 0.91, MgO 0.09, UO_3 56.72, As_2O_5 21.31, P_2O_5 0.22, SiO_2 0.09, H_2O 14.61 (de l'analyse thermique), et mène à la formule empirique $(Ni_{0.82}Co_{0.12}Mg_{0.02})_{\Sigma 0.96}(UO_2)_{2.01}[(AsO_4)_{1.88}(PO_4)_{0.03}(SiO_4)_{0.02}]_{\Sigma 1.93}•8.21H_2O$ (sur une base de 20 atomes O,OH). Selon l'analyse thermique, la métarauchite se déshydrate en plusieurs étapes, et la perte totale en poids est 14.61%, ce qui correspond à 8.21 H_2O. Nous en avons étudié le spectre infrarouge et le spectre Raman. Nous avons attribué les vibrations d'étirement et d'articulation des unités $(UO_2)^{2+}$, $(AsO_4)^{3-}$ et H_2O de façon provisoires. De plus, nous avons évalué les longueurs des liaisons U–O de l'uranyle et des liaisons hydrogène O–H...O à partir des spectres. La métarauchite a été découverte dans la veine Schweitzer, camp minier de Jáchymov (St. Joachimsthal) en République Tchèque (localité type), en association avec la métazeunerite, l'érythrite et le gypse. Nous présentons aussi certaines données pour la métarauchite de Schneeberg, en Allemagne, associée à la métanováčekite riche en nickel et la métazeunerite.

(Traduit par la Rédaction)

Mots-clés: nouvelle espèce minérale, métarauchite, uranyle, diffraction X sur poudre, données de microsonde électronique, analyse thermique, spectroscopie infrarouge, spectroscopie de Raman, liaisons uranyle, liaisons hydrogène, Jáchymov, République Tchèque, Schneeberg, Allemagne.

Introduction

Metarauchite is a new member of the autunite group, found at the Jáchymov ore district (type locality), Czech Republic and in Schneeberg, Germany. It is a Ni- and As-dominant member of the group of hydrated uranyl arsenates and phosphates with the autunite-type sheet containing divalent cations in their interlayer. Metarauchite has been approved by the Commission of New Minerals, Nomenclature and Classification of the IMA (# 2008–50). The mineral is named after Czech mineral collector Luděk Rauch (1.7.1951 – 5.12.1983), who died in the Jáchymov mines during mineral prospecting. The holotype is deposited in the mineralogical collection of the Natural History Museum, National Museum, Prague, Czech Republic under the catalogue number P1p 19/2008.

Background Information

The group of hydrated uranyl arsenates and phosphates containing divalent transition metal cations in their interlayer are represented by the general formula $^{[6]}M^{2+}(UO_2)_2(TO_4)_2•nH_2O$ (*T* = As, P), where *n* is mostly 12, 10 or 8 (Locock 2007a). Divalent cations including Cu, Co, Ni, Fe, Mn and Zn occupy sixfold-coordinated M^{2+} sites. To date, only arsenic and phosphorus have been found in significant amounts occupying the *T* sites. Recently, new crystallographic data for some synthetic analogues of these minerals were reported by Locock *et al*. (2004). They presented crystal structures of kahlerite, $Fe[(UO_2)_2(AsO_4)_2]•10H_2O$, nováčekite II, $Mg[(UO_2)_2(AsO_4)_2]•10H_2O$, metakahlerite, $Fe[(UO_2)_2(AsO_4)_2]•8H_2O$, metakirchheimerite, $Co[(UO_2)_2(AsO_4)_2]•8H_2O$, and unnamed, unapproved minerals, dodecahydrates and decahydrates and phosphates of uranyl and nickel, $Ni[(UO_2)_2(PO_4)_2]•10–12H_2O$, kirchheimerite, $Co[(UO_2)_2(AsO_4)_2]•10H_2O$, and a phase related to lehnerite, $Mn[(UO_2)_2(AsO_4)_2]•8H_2O$. The natural zinc uranyl arsenate of this group is represented by the mineral metalodèvite, $Zn[(UO_2)_2(AsO_4)_2]•8H_2O$ (Agrinier *et al*. 1972, Plášil *et al*. 2010). Naturally occurring nickel uranyl arsenate hydrate, which corresponds to metarauchite, was reported for the first time by Ondruš *et al*. (1997a) as an unnamed phase from the Jáchymov ore district. Synthetic nickel uranyl arsenate octahydrate was prepared by Nabar & Iyer (1977), and the heptahydrate, later by Vochten & Goeminne (1984).

According to Locock *et al*. (2004), there are three stable hydration states for the hydrated uranyl phosphates and arsenates of divalent transition metals: the dodecahydrate, decahydrate and octahydrate. The symmetry of these phases depends on the hydration state: triclinic for 12 H_2O, monoclinic for 10 H_2O, and

triclinic for 8 H_2O. The position of the basal diffraction maximum in the powder pattern corresponds to the hydration state of the each phase: d_{basal} ~11 Å for the dodecahydrate, ~10 Å for the decahydrate and ~8.5 Å for the octahydrate. Corner-sharing uranyl-hosting tetragonal bipyramids linked to arsenate or phosphate tetrahedra result in autunite-type sheets (Locock 2004, 2007a, 2007b). In the case of octahydrates, five H_2O groups octahedrally coordinate divalent cations in the interlayer position, whereas the sixth vertex is an apical atom of oxygen shared with the uranyl square bipyramid (Locock 2007a). Interlayer cations of similar size lead to identical crystal structures (Locock 2007a).

Occurrence and Associated Minerals

Metarauchite, commonly associated with metazeunerite, erythrite and gypsum, covers a surface of strongly altered aggregates of primary ore with relics of uraninite, arsenopyrite and nickelskutterudite and traces of native bismuth at the Schweitzer vein on the second level of the Eduard mine. It is located in the northern part of the Jáchymov ore district, northwestern Bohemia, Czech Republic. Jáchymov (St. Joachimsthal), world-classic example of Ag + As + Co + Ni ± Bi and U mineralization, was described in detail by Ondruš *et al*. (1997a, 1997b, 2002, 2003a, 2003b, 2003c, 2003d). Within the Jáchymov ore district, more than 380 mineral species have been described to date, and for 30 of them, Jáchymov is the type locality.

Metarauchite from Schneeberg was found at the Adam Heber mine, Neustädtel, Schneeberg district, Germany. The history of mining, geology, economic geology, mineralogy and general literature concerning the Schneeberg district has been extensively reviewed by Lahl (2005), Herrmann (2005), Massanek & Michalski (2005), Weiss (2005), Gröbner & Kolitsch (2005) and Thalheim (2005). Metarauchite was found at the "Gang Adam Heber Flache" in a strongly oxidized vein material, at a depth of 10–12 m.

Physical Properties

Metarauchite from Jáchymov forms thick tabular crystals with a prevalence of the pinacoid (011); these crystals are multiply twinned along {011} (Figs. 1, 2). Yellow to light greenish yellow crystals, up to 0.8 mm in size, are transparent to translucent with a vitreous luster and locally pearly on (011). They have a light green to pale yellow streak. The crystals are very brittle, with perfect (011) cleavage and an uneven fracture. The Mohs hardness is about 2. Metarauchite does not exhibit fluorescence either in short- and long-wavelength ultraviolet radiation. The density of metarauchite could not be measured because of relatively small size of most crystals; hence only the calculated density from the unit-cell parameters and empirical formula was obtained, giving the value 3.81 g•cm^{-3}. The crystals are readily soluble in cold 10% HCl acid. Metarauchite is biaxial negative, $\alpha = 1.625(3)$, $\beta \approx \gamma = 1.649$ (1.646–1.651,

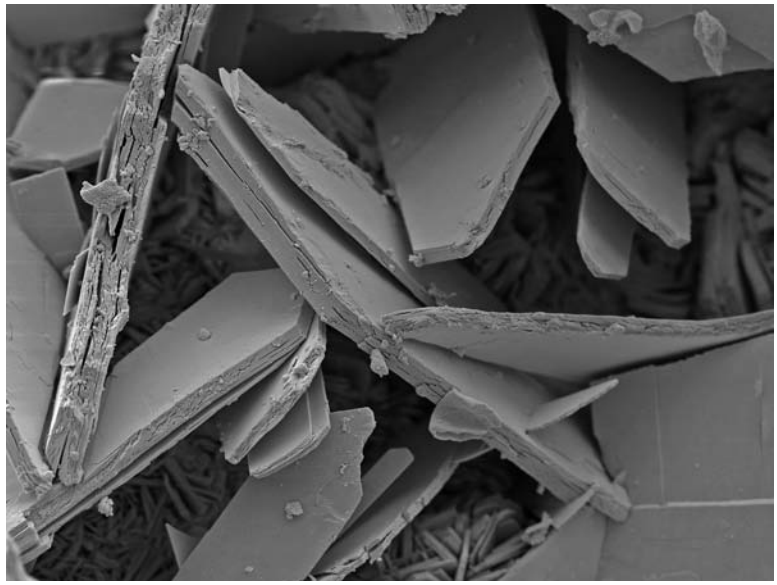

FIG. 1. Group of tabular crystals of metarauchite showing the dominant face (011) and cracks corresponding with its perfect cleavage. The width of SE image is 800 μm. Photo by J. Sejkora (JEOL JSM–6380).

seven measurements; 589 nm); calculated $2V = 52°$ with $\beta = 1.646$, $\gamma = 1.651$ and to 23° with $\beta = 1.649$, $\gamma = 1.650$. Metarauchite it is not pleochroic. The Gladstone–Dale compatibility index, calculated on the basis of incomplete optical data, is 0.03, *i.e.,* excellent (for a compatibility of 0.00, the mean N is 1.661).

Metarauchite from Schneeberg occurs as isolated crystals, up to 1 mm in diameter (Fig. 3), or as aggregates, scattered on fractures or small vugs in a matrix of vuggy quartz. Here, metarauchite is associated with Ni-bearing metanováčekite and metazeunerite; occasionally, pharmacosiderite was found on metarauchite crystals. No primary mineral was observed with the metarauchite samples, but siliceous epimorphs (void moulds) after skutterudite-like crystals were found in some specimens.

X-Ray Diffraction

Attempts to obtain proper single-crystal X-ray-diffraction data suitable for solving of the crystal structure of metarauchite were unsuccessful because of the multiple intergrowths of the crystals. Therefore, the unit-cell parameters were refined from powder-diffraction data.

A hand-picked sample of metarauchite from Jáchymov was used for the X-ray powder-diffraction experiment. The continuous mode of the PANalytical X'Pert Pro diffractometer operating at 40 kV and 30 mA equipped with an X'Celerator detector and secondary graphite monochromator was used. The aggregates of crystals of metarauchite were mildly ground and mixed with a portion of glass powder to randomize the preferentially oriented crystallites and to lower the absorption. The powder X-ray-diffraction pattern for the unit-cell parameters refinement was collected between 5° and 100° 2θ using Cu$K\alpha$ radiation in Bragg–Brentano geometry, with an integrated step of width 0.02° and a counting time of 1200 s per step. The position of each diffraction maximum was refined using a Pearson VII profile shape-function with the Xfit software (Cheary & Coelho 1996). For the refinement of unit-cell parameters, the Celref software (LMGP Suite of Programs for the Interpretation of X-ray Experiments, by Jean Laugier and Bernard Bochu, ENSP Laboratoire des Matériaux et du Génie Physique, BP 46, F–38042 Saint Martin d'Hères, France. http://www.inpg.fr/LMGP and http://www.ccp14.ac.uk/tutorial/lmgp/) was used. The unit-cell parameters were refined on the basis of 52 diffraction maxima obtained from the profile fit (Table 1). The powder pattern was indexed on the basis of the calculated diffraction-pattern of synthetic metakirchheimerite (Locock *et al*. 2004), as the ionic radii of Ni and Co are similar (Shannon 1976). The powder X-ray-diffraction pattern of metarauchite from Schneeberg was collected on Bruker D8 Advanced diffractometer equipped with LynxEye detector, operating at 40 kV and 40 mA. A primary optics consisting of a focusing Göbel mirror with a fixed slit of 0.1 mm was used to produce a convergent beam of Cu$K\alpha_{1,2}$ radiation. The

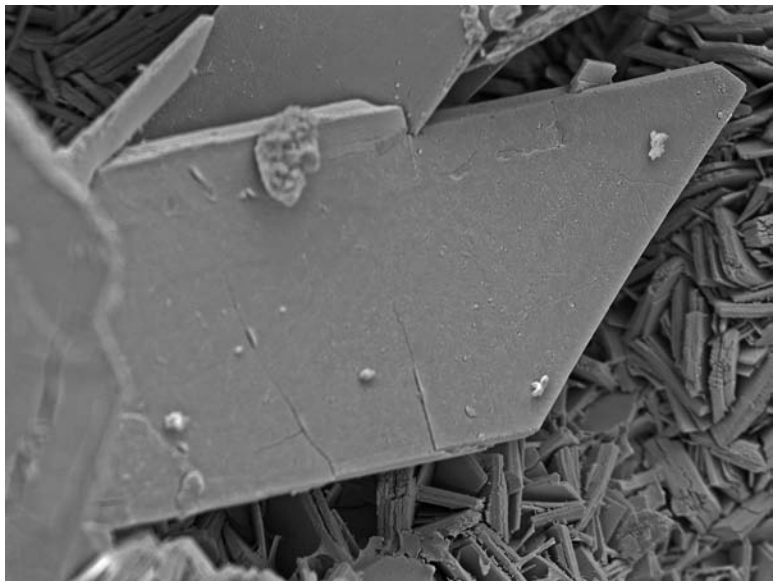

Fig. 2. Detail of well-shaped crystal of metarauchite growing on fine crystalline aggregates of the same mineral. The width of SE image is 450 μm. Photo by J. Sejkora (JEOL JSM–6380).

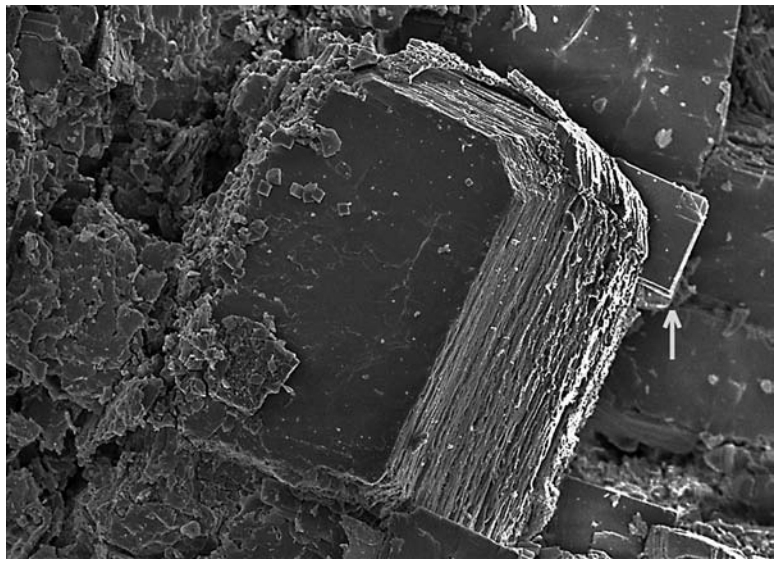

FIG. 3. Typical aggregate of metarauchite crystals with a small tetragonal crystal of metazeunerite (arrow) from Schneeberg. Width of SE image is 500 μm. Photo by J. Vi∞als.

powder sample of metarauchite was mixed with a glass powder to randomize the crystallites and loaded into glass capillary of a diameter of 0.3 mm. The powder X-ray-diffraction pattern for the unit-cell refinement was collected between 6° and 70° 2θ with a step size of 0.015° and variable counting time (starting 5 s, ending 79 s per step). The unit-cell parameters of metarauchite from Schneeberg were refined by the Rietveld method with the Topas software (Bruker). As a structural model, crystallographic data for the synthetic metakirchheimerite (Locock *et al*. 2004) were used. The site occupancy for Co was modified for Ni respecting the chemical composition. The coordinates of the atoms were not refined prior to the data-quality from the in-house powder diffractometer. The data pertinent to the collection and refinement are listed in Table 2.

The powder X-ray-diffraction pattern of metarauchite from Jáchymov is strongly affected by preferred orientation caused by the excellent (011) cleavage. The diffraction profiles at higher diffraction-angles are thus only poorly described, except for the 0*kl* family. The refined unit-cell parameters (Table 3) are consistent with those given by Locock *et al*. (2004) for the synthetic analogues of this mineral group. The powder X-ray-diffraction pattern presented has significantly higher FWHM resolution (owing to the method used) than the one submitted with the new mineral proposal; therefore, the refined unit-cell parameters are slightly different from the data at www.pubsites.uws.edu.au\ima–cnmnc.

TABLE 1. POWDER X-RAY-DIFFRACTION DATA FOR METARAUCHITE FROM JÁCHYMOV

I_{obs}	h	k	l	d_{obs}	d_{calc}	I_{obs}	h	k	l	d_{obs}	d_{calc}
100	0	1	1	8.54	8.55	1	2	3	1	2.570	2.572
3	1	1	1	5.96	5.96	1	2	$\bar{1}$	3	2.532	2.534
6	$\bar{1}$	1	1	5.09	5.07	3	$\bar{1}$	3	3	2.505	2.507
5	$\bar{1}$	$\bar{1}$	1	5.06	5.05	2	0	4	2	2.379	2.380
1	1	0	2	4.93	4.93	2	$\bar{1}$	1	5	2.375	2.377
1	1	$\bar{1}$	1	4.80	4.79	1	0	$\bar{3}$	$\bar{3}$	2.272	2.272
8	0	2	0	4.67	4.67	1	1	$\bar{2}$	4	2.253	2.257
49	0	2	2	4.28	4.28	4	2	3	4	2.245	2.246
<1	1	2	0	4.14	4.15	32	0	4	4	2.138	2.138
2	$\bar{1}$	$\bar{1}$	2	3.981	3.979	3	$\bar{1}$	3	5	2.053	2.054
12	1	2	2	3.957	3.959	2	1	$\bar{1}$	$\bar{4}$	1.9620	1.9605
<1	$\bar{1}$	2	1	3.711	3.698	3	1	5	3	1.8916	1.8929
2	0	2	3	3.595	3.591	3	1	4	6	1.8088	1.8096
4	0	$\bar{1}$	3	3.573	3.570	1	$\bar{1}$	5	1	1.7861	1.7867
4	2	0	0	3.547	3.548	4	2	$\bar{4}$	2	1.7106	1.7092
3	2	1	1	3.484	3.485	3	$\bar{1}$	4	6	1.6800	1.6788
8	1	2	3	3.431	3.429	<1	3	3	6	1.6467	1.6455
12	$\bar{1}$	2	2	3.417	3.424	2	0	6	2	1.6015	1.6011
	0	$\bar{2}$	2		3.411	2	1	6	4	1.5672	1.5674
10	0	3	1	3.201	3.203	2	1	6	0	1.5625	1.5622
	0	0	4		3.195	2	1	5	7	1.5086	1.5079
2	$\bar{2}$	1	1	3.100	3.103	1	0	5	7	1.4896	1.4906
2	1	$\bar{2}$	2	3.009	3.012	1	$\bar{1}$	6	4	1.4650	1.4657
8	0	2	4	2.977	2.980	1	1	6	6	1.4435	1.4435
1	0	$\bar{3}$	1	2.880	2.875	1	0	6	6	1.4251	1.4252
1	0	3	3	2.850	2.850	<1	1	8	8	1.0835	1.0833
5	1	3	3	2.807	2.808	1	0	8	8	1.0691	1.0689

d values are quoted in Å.

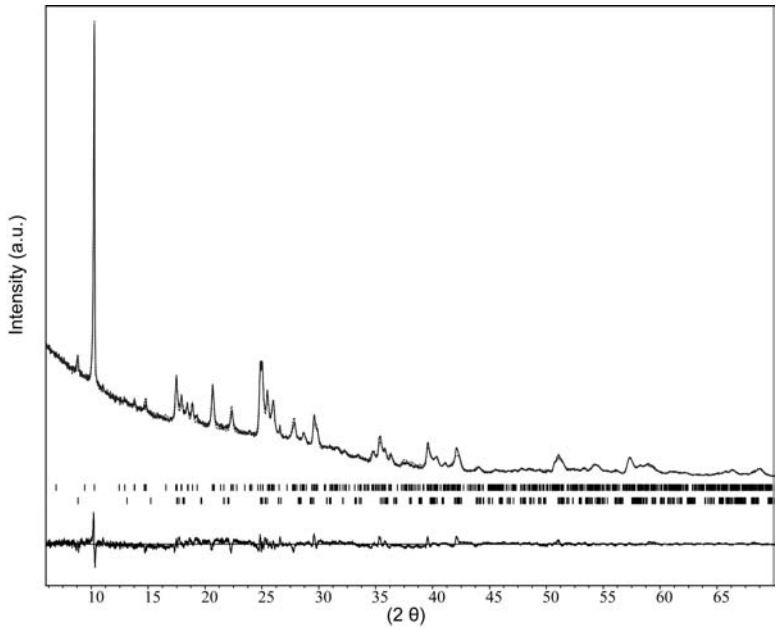

FIG. 4. Rietveld plot of observed (solid line), calculated (dotted line) and difference (line at the bottom) profiles for metarauchite sample from Schneeberg. The vertical bars indicate positions of the Bragg reflections: for metarauchite (upper) and for unnamed phase (corresponding to the crystallographic properties of synthetic nováčkeite II of Locock *et al*. 2004).

TABLE 2. DETAILS CONCERNING DATA COLLECTION AND RIETVELD REFINEMENT OF METARAUCHITE FROM SCHNEEBERG

Data collection	
Radiation type, source	X-ray, Cu$K\alpha_{1,2}$
Geometry, primary optics	Debye–Scherrer, focusing Göbel mirror
Range (2θ)	6–70°
Step size (°)	0.016
Refinement	
Background	Chebychev (6th order)
Zero-shift (cylindrical sample)	–0.07
Asymmetry	Full axial convolution
Peak type	Pseudo-Voigt
Reliability factors	
R_{Bragg}	0.018
$R_{p'}$	0.187
$R_{wp'}$	0.158
GOF	3.05

$R_{p'}$ and $R_{wp'}$ are background-corrected indices of agreement; reliability factors are defined according to Young (1993); the zero-error correction is after Sabine *et al.* (1998).

The final plot of the Rietveld refinement of metarauchite from Schneeberg is depicted in the Figure 4. The refinement revealed that there is an additional phase present in the powder-diffraction pattern of the sample, with $d_{basal} \approx 10$ Å. This phase was introduced into the fit using crystallographic parameters of Locock *et al*. (2004) for the synthetic decahydrate, metanováčekite II, and it corresponds to an unapproved higher hydrate of metarauchite. Its unit-cell parameters for the monoclinic space-group $P2_1/n$ are *a* 7.15(1), *b* 20.02(2), *c* 7.141(9) Å, β 90.2(2)°, with a unit-cell volume *V* of 1022(2) Å^3. This value is in agreement with the volumes reported by Locock *et al*. (2004) for decahydrates. The proportion of the decahydrate in the mixture is based on the Rietveld refinement is approximately 7%. An overview of the refined unit-cell parameters for the group of octahydrates is listed in Table 3. The unit-cell parameters of metarauchite from Schneeberg are similar to those of the sample from Jáchymov.

CHEMICAL COMPOSITION AND THERMAL ANALYSIS

The chemical composition of metarauchite was studied using a Cameca SX100 electron microprobe (Laboratory of Masaryk University and Czech Geolog-

ical Survey, Brno, R. Škoda, analyst) operated in the wavelength-dispersion mode. We applied an acceleration voltage of 15 kV, a current of 2 nA, and a beam diameter of 20 μm. The following X-ray lines and standards were selected to minimize line overlaps: *K*α lines: P (fluorapatite), Fe (andradite), Mg ($MgAl_2O_4$), Si (sanidine), Zn (ZnO), Ni (metal Ni), Co (metal Co); *L*α lines: As (InAs); *M*β lines: U (metal U). Peak counting times (CT) were 10–20 seconds for major elements, 40–60 seconds for minor to trace elements, and the counting time for background was ½ CT. The measured intensities were converted to element concentrations using the PAP program (Pouchou & Pichoir 1985).

As the Schneeberg material exhibits important Mg-for-Ni substitution, an additional set of analyses was performed in order to establish its extent. A total of 25 crystals were examined, from which 74 spot analyses corresponds to the metarauchite – metanováčekite – metakirchheimerite series. This study was carried out on a Cameca SX50 (Serveis Cientifictécnis University of Barcelona, X. Llovet, analyst) operating at an acceleration voltage of 20 kV, 6 nA current and 5 μm beam diameter. The counting time CT was 20 s. The following X-ray lines and standards were used: *K*α: Na (albite), Mg (periclase), Si (diopside), S (barite), P (fluorapatite), Ni (NiO), Co (metal Co), Cu (Cu_2O), Fe (Fe_2O_3); *L*α: As (GaAs); *M*α: U (UO_2). The measured intensities were converted to element concentrations using the PAP program (Pouchou & Pichoir 1985).

Metarauchite from Jáchymov is the Ni,As-dominant member of the octahydrates belonging to the autunite-group minerals, with the general formula $M^{2+}(UO_2)_2(TO_4)_2$•8 H_2O (where *T* = As or P). The octahedrally coordinated M^{2+} position is in part replaced by Co (up to 0.15 *apfu*) and Mg (up to 0.24 *apfu*) along with dominant Ni. In the tetrahedral sites, minor anionic groups $(PO_4)^{3-}$ (up to 0.32 *apfu*) and $(SiO_4)^{4-}$ (up to 0.16 *apfu*) are present. The empirical formula of metarauchite from Jáchymov calculated on the basis of 20 O, OH (mean result of 13 point analyses: Table 4) is $(Ni_{0.82}Co_{0.12}Mg_{0.02})_{\Sigma 0.96}(UO_2)_{2.01}[(AsO_4)_{1.88}(PO_4)_{0.03}(SiO_4)_{0.02}]_{\Sigma 1.93}$•8.21 H_2O. The sum of the cations is close to be 1 *apfu*, which is in accordance to the ideal formula of the autunite-group minerals; this suggests correctness of the chemical data for metarauchite.

The chemical composition of metarauchite from Schneeberg exhibits more extensive substitution trends at both cationic and anionic sites (Table 4, Figs. 5 and 6). Cationic substitution trends tend toward metanováčekite (Mg, up to 0.50 *apfu*), metakirchheimerite (Co, up to 0.21 *apfu*) and metalodèvite (Zn, up to 0.05 *apfu*) in all metarauchite samples (Fig. 5) and complete solid-solution in the series metarauchite–metanováčekite was confirmed. Contrasting with these extensive substitutions, Cu was not detected in significant concentration in spite of the Cu^{2+}-rich environment. Copper is incorporated into metazeunerite, which commonly forms an intergrowth with the Schneeberg metarauchite. These intergrowths are constrained by a different arrangement of the interlayer in metazeunerite, where coordination polyhedra are strongly distorted owing to the Jahn–Teller effect (Locock & Burns 2003). Also in the anionic position, extensive substitutions, namely in the $(PO_4)^{3-}$ component, up to 0.60 *apfu* $(PO_4)^{3-}$ (Fig. 6), were observed. This component corresponds to the substitution between metarauchite and synthetically prepared hydrated Ni uranyl phosphate (Vochten & Goeminne 1984). The presence of minor $(SiO_4)^{4-}$, up to 0.07 *apfu* at Schneeberg, is surprising, as in the Jáchymov

TABLE 3. SELECTED DATA FOR METARAUCHITE AND RELATED PHASES (BOTH SYNTHETIC AND NATURAL)

Mineral	meta-rauchite	meta-rauchite	meta-kirchheimerite	meta-lodèvite	meta-nováčekite	meta-kirchheimerite	meta kahlerite	–
Locality	Jáchymov	Schneeberg	Jáchymov	Příbram	Jáchymov	synthetic	synthetic	synthetic
Reference	this work	this work	Plášil *et al.* (2009)	Plášil *et al.* (2010)	Plášil (2009)	Locock *et al.* (2004)	Locock *et al.* (2004)	Locock *et al.* (2004)
M^{2+} (ideal)	Ni	Ni	Co	Zn	Mg	Co	Fe	Mn
M^{2+} (meas.)	$Ni_{0.81}Co_{0.13...}$	$Ni_{0.77}Mg_{0.13...}$	$Co_{0.53}Mg_{0.25...}$	$Zn_{0.72}Fe_{0.10}$...	$Mg_{0.65}Ni_{0.27}$...	-	-	-
T site	As	As, P, Si	As	As, P	As	As	As	As
n H_2O	8.21	8	8	8	8	8	8	8
d_{011} (Å)	8.54	8.60	8.68	8.71	8.64	8.61	8.66	8.76
Space group	$P\bar{1}$	$P\bar{1}$	$P\bar{1}$	$P\bar{1}$	$P\bar{1}$	$P\bar{1}$	$P\bar{1}$	$P\bar{1}$
a (Å)	7.194(4)	7.197(3)	7.210(4)	7.143(3)	7.201(5)	7.1955(3)	7.2072(3)	7.2244(5)
b (Å)	9.713(5)	9.759(4)	9.771(6)	9.773(5)	9.755(7)	9.7715(4)	9.8242(4)	9.9170(8)
c (Å)	13.201(9)	13.255(5)	13.252(9)	13.224(5)	13.27(6)	13.2319(6)	13.2708(6)	13.337(1)
α (°)	75.79(3)	75.59(1)	75.39(4)	75.10(3)	75.54(5)	75.525(1)	75.370(1)	75.012(2)
β (°)	83.92(5)	83.88(1)	83.94(6)	81.90(3)	83.84(6)	84.052(1)	84.024(1)	84.136(2)
γ (°)	81.59(4)	81.62(1)	81.88(6)	83.70(4)	81.87(6)	81.661(1)	81.839(1)	81.995(2)
V (Å^3)	882.2(9)	889.7(6)	892(1)	880.6(8)	891(1)	889.08(7)	897.68(7)	911.83(12)
Z	2	2	2	2	2	2	2	2

samples. According to Locock (2007a), this anionic group is not predicted to be involved in the structure sheets of the autunite topology. However, the concentrations of $(SiO_4)^{4-}$ obtained are reliable and were found in almost all point analyses. The mechanism of incorporation and the role of $(SiO_4)^{4-}$ in the crystal structure remain unclear. The empirical formula of metarauchite from Schneeberg (mean of 8 Ni-rich samples, on the basis of 20 O,OH) is $(Ni_{0.74}Mg_{0.13}Co_{0.11}Zn_{0.02})_{\Sigma 1.00}(UO_2)_{2.01}[(AsO_4)_{1.62}(PO_4)_{0.28}(SiO_4)_{0.03})]_{\Sigma 1.93}\bullet 7.99H_2O$.

Thermal analysis

A thermal analysis of the Jáchymov sample was performed on a Stanton Redcroft Thermobalance TG 750, at the heating rate of 10°C•minute^{-1} in dynamic air atmosphere; the flow rate was 10 mL•minute^{-1}, and the sample weight was 0.2 mg.

The thermal decomposition curve (TG) of the Jáchymov sample suggests that release of the molecular H_2O from the interlayer proceeds in several steps between ~20° and 320°C. The total weight loss, 14.61 wt.%, corresponds to 8.21 moles of H_2O and is consistent with the theoretical content of eight molecules; the deviation is mainly due to instrumental errors, reflecting the small weight of the sample.

The dehydration can be expressed as follows: $8H_2O$ phase → $7H_2O$ phase (at 95°C, weight loss 2.44 wt.% corresponding to 1.37 H_2O) → $5H_2O$ phase (at 110°C, 3.50 wt.%, ~1.97 H_2O) → $3H_2O$ (180°C, 3.82 wt.%, ~2.14 H_2O) → anhydrous phase (to ~320°C, 4.85 wt.%, ~2.73 H_2O). The remnants after heating were checked by powder X-ray diffraction. The pattern obtained belongs to an unknown crystalline phase (Table 5), resembling that reported by Chernorukov *et al.* (1998).

Vibration Spectroscopy: Tentative Assignments

The infrared spectra of the samples of metarauchite were recorded by the micro-diffuse-reflectance method (DRIFTS) on a Nicolet Magna 760 FTIR spectrometer (range 4000–600 cm^{-1}, resolution 4 cm^{-1}, 128 scans, Happ–Genzel apodization) equipped with a Spectra Tech InspectIR micro-FTIR accessory. Samples were

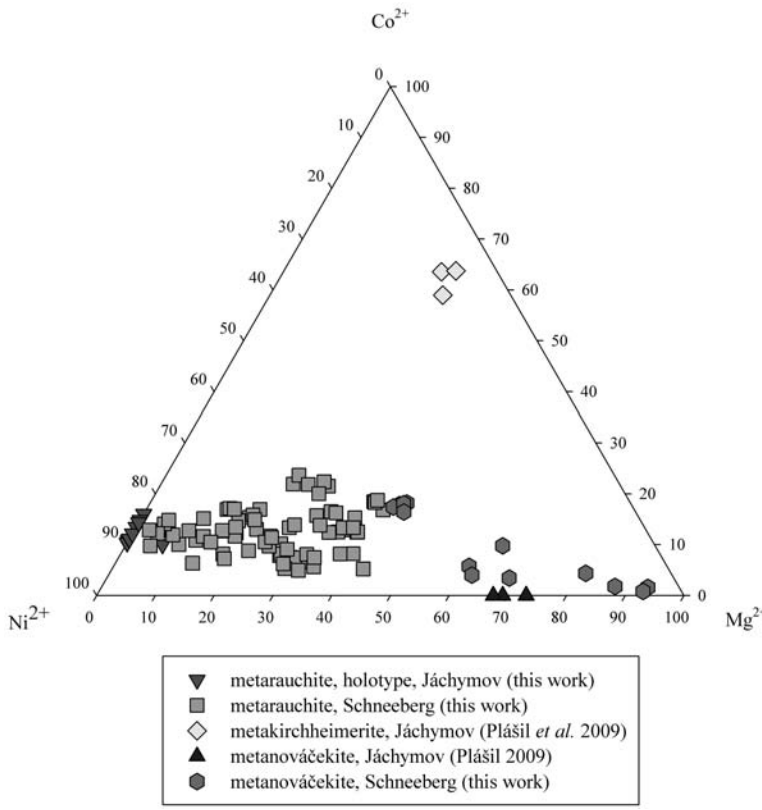

FIG. 5. Plot of the M^{2+} site-occupancy (atom proportions) in metarauchite and related minerals.

mixed with KBr without using pressure, to avoid dehydration or solid-state reactions, and immediately measured. The same KBr was taken as a reference.

The Raman spectra were collected on the multichannel Raman microspectrometer (Renishaw/InVia/Reflex) coupled with a Peltier-cooled CCD detector. Excitation was provided by the 514.5 nm line of a continuous-wave 10 mW Ar ion laser (laser set to 2% of its power). The samples were scanned from 200 to 1800 cm^{-1} and from 1800 to 3800 cm^{-1} at a spectral resolution of 2 cm^{-1}. The counting time for acquisition of each Raman spectrum was 10 seconds, and 10 scans were accumulated for each experimental run to provide a better signal-to-noise ratio. Multiple-spot analyses on different areas of the same sample produced similar spectra and confirmed the spectral reproducibility. The manipulation and processing of both spectra were performed using the OMNIC SPECTRAL TOOLS software. The peak positions of single bands were determined by fits of Gaussian–Lorentzian profile shape function; we refined the position of the band, its height and FWHM. Band positions are summarized in Table 6.

The infrared spectrum of the holotype sample of metarauchite from Jáchymov (Fig. 7) is similar to those published by Vochten & Goeminne (1984), Ondruš *et al*. (1997a), Čejka (1999) and Chernorukov *et al*. (1998, 2000). A detailed description, molecular and factor-group analysis of both infrared and Raman spectra of natural hydrated uranyl arsenates including metarauchite will be published separately (Plášil *et al*., in prep.).

Stretching O–H, bending H–O...H vibrations

A broad, relatively intense band occurring in the infrared spectrum of metarauchite between 3200 and ~3500 cm^{-1} was assigned to ν OH stretching vibrations of H_2O molecules (Figs. 7, 8). The character of this broad band reflects the presence of a hydrogen bond

TABLE 4. CHEMICAL COMPOSITION OF METARAUCHITE FROM JÁCHYMOV AND SCHNEEBERG (Ni-RICH SAMPLES)

		Jáchymov, holotype		Schneeberg	
	Ideal composition	Mean	Range (13 analyses)	Mean	Range (8 analyses)
MgO wt%	0.00	0.09	0.00 – 0.24	0.50	0.17 – 0.88
CoO	0.00	0.91	0.71 – 1.13	0.81	0.57 – 1.09
NiO	7.32	6.05	5.58 – 7.10	5.48	4.81 – 6.86
ZnO	0.00	0.00	–	0.14	0.00 – 0.42
SiO_2	0.00	0.09	–	0.16	0.00 – 0.42
P_2O_5	0.00	0.22	0.12 – 0.32	1.96	0.64 – 3.83
As_2O_5	22.52	21.31	19.87 – 23.22	18.34	14.03 – 23.61
UO_3	56.04	56.72	55.65 – 60.97	58.42	59.64 – 64.49
H_2O	14.12*	14.61#		14.19$	
Total	100.00	100.00		100.00	
Mg *apfu*		0.02		0.13	
Co		0.12		0.11	
Ni		0.82		0.74	
Zn		–		0.02	
Σ*A* site		0.96		1.00	
Si		0.02		0.03	
As		1.88		1.62	
P		0.03		0.28	
Σ*T* site		1.93		1.93	
U		2.01		2.07	
H_2O		8.21		7.99	

* The theoretical content of H_2O groups derived from 8 moles of H_2O in ideal formula of metarauchite. # H_2O content derived from thermal analysis; mean normalized with the total of 100 wt.% after supply by the thermal analysis supplement. $ H_2O content based on theoretical content of 8 H_2O molecules in ideal formula of metarauchite, mean normalized with the total of 100 wt.% after supply by ideal H_2O content.

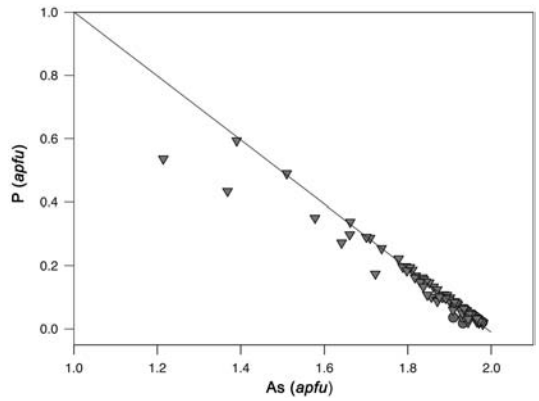

FIG. 6. Plot of anion-site occupancy (*apfu* contents) in metarauchite samples from Jáchymov (circle symbols) and Schneeberg (triangles). The deviations from the ideal correlation corresponding to solid line As + P = 2 *apfu* is caused by the Si contents in the samples.

TABLE 5. POWDER X-RAY-DIFFRACTION DATA FOR THE RESIDUE AFTER TG ANALYSIS OF METARAUCHITE FROM JÁCHYMOV, IN COMPARISON WITH THE DATA OF CHERNORUKOV *et al.* (1998)

d_{obs}	I_{rel}	d_{obs}*	I_{rel}*	d_{obs}	I_{rel}	d_{obs}*	I_{rel}*
8.71	10	-	-	2.334	13	2.350	33
-	-	4.995	11			2.270	12
4.67	100	4.683	100			2.103	33
4.37	7	4.301	52			1.916	34
4.28	8	-	-			1.836	5
3.568	4	3.576	95			1.784	9
-	-	3.507	33			1.746	9
3.141	6	3.116	18			1.710	5
-	-	3.003	9			1.616	11
-	-	2.705	4			1.583	8
-	-	2.567	6	1.5560	10	1.555	9
-	-	2.491	15				

* Data of Chernorukov *et al.* (1998).

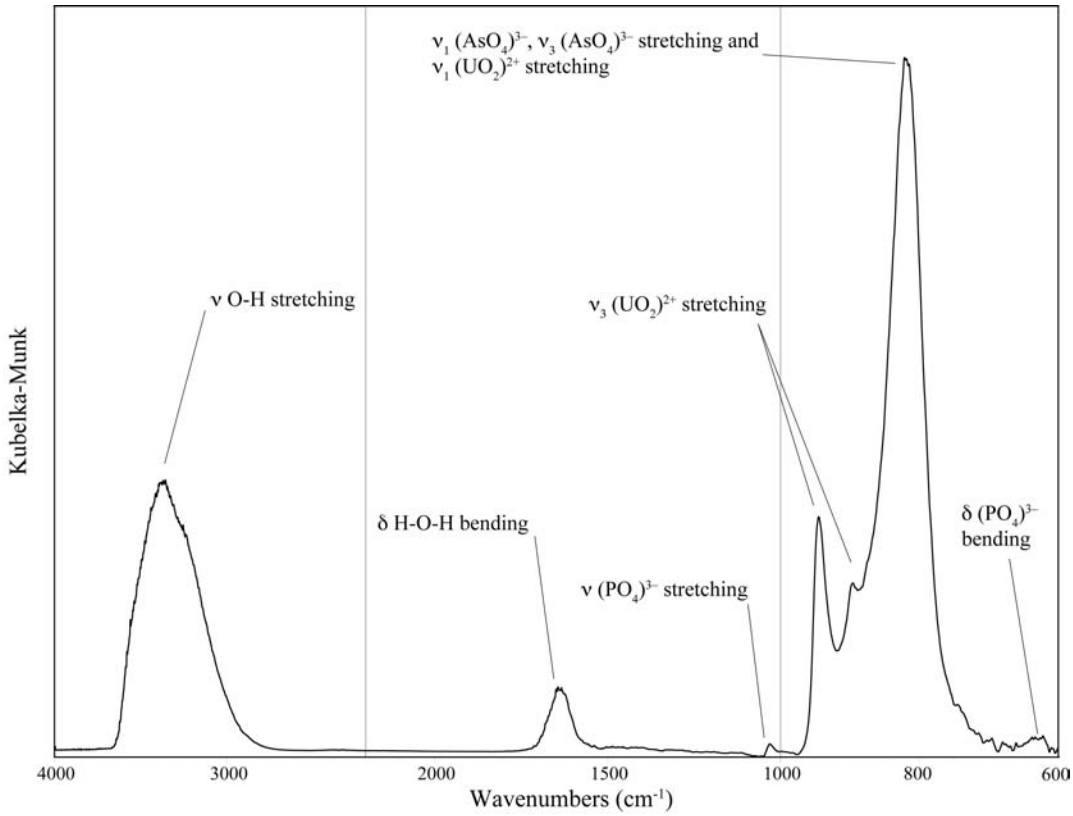

FIG. 7. The DRIFTS spectrum of metarauchite from Jáchymov with assigned bands and regions of vibration modes.

network in the crystal structure of metarauchite. Based on the correlation curves between the wavenumber of the O–H stretching vibrations and O–H bond length (Libowitzky 1999), it is possible to infer the approximate lengths of hydrogen bonds. The possible range of hydrogen-bond lengths in metarauchite varies from 2.7 to 3.1 Å. Hydrogen-bond lengths in a synthetic sample of metakirchheimerite inferred from the structure analysis varies from 2.7 to 3.2 Å (Locock *et al.* 2004). We attribute an infrared band of weak intensity occurring at 1640 cm^{-1} to the ν_2 (δ) bending vibration of H_2O molecules (Fig. 7). The asymmetry of the band suggests a splitting of the vibration. The weak band located at 745 cm^{-1} may be attributed to librations of H_2O molecules (Čejka 1999).

Vibrations of the uranyl $(UO_2)^{2+}$ and $(AsO_4)^{3-}$ groups

The departure from ideal $D_{\infty h}$ symmetry of the uranyl ion $(UO_2)^{2+}$ in the crystal structure of metarauchite, which is caused by the constraints of both the site and the factor group, is conducive to the splitting (and multiplying) of degenerate vibrations and the activation of inactive vibrations both in infrared and Raman spectra. Lowering of the ideal symmetry T_d of the $(AsO_4)^{3-}$ group to the symmetry of the site (C_1) or the factor group (C_i) tends toward the same feature as presented in the case of the uranyl ion.

The U–O stretching vibrations ν_1 and ν_3 occur in the region 1000–750 cm^{-1} (Čejka 1999). In the case of our mineral, overlapping of the superimposed stretching modes of uranyl and the split of stretching modes of the $(AsO_4)^{3-}$ groups located in the same region may be expected (Figs. 7, 8). This feature makes the interpretation of the spectra and assignment very difficult. A possible way to resolve the overlapping peaks in order to make a tentative assignment is *via* inferences about the wavenumbers of uranyl-stretching vibration from the known U–O bond-lengths given from single-crystal data and comparison with the experimental spectrum and the decomposed peaks, respectively. In order to infer the wavenumbers of the U–O stretch, the empirical relations given by Bartlett & Cooney (1989) were applied.

The ν_1 $(AsO_4)^{3-}$ stretching vibration has less energy; consequently, its position should be shifted to lower wavenumbers compared to ν_3 $(AsO_4)^{3-}$. The same rule applies for the stretching vibrations of the uranyl ion. The activity predicted from the factor-group analysis will not match exactly the experimental spectra. For example, ν_1 $(AsO_4)^{3-}$ may be present in the infrared spectrum as a shoulder component, but ν_3 $(AsO_4)^{3-}$ should not be evident in the Raman spectrum. The other problem could be the polarization of symmetric bands (A_g), with variable intensity. For this reason, these bands can in some cases be easily identified, but only in the case of manipulation of simple crystals of appropriate quality and size.

The superposition of the Raman and the infrared spectrum is clearly visible in Figure 9. Figure 10 represents a decomposition of the Raman spectrum of metarauchite in the region ~960–600 cm^{-1}; it displays seven reliable Raman bands, at 898, 893, 884, 878, 817, 804, 785 and 771 cm^{-1}. These eight Raman bands in the range from 898 to 771 cm^{-1} may be assigned to the overlapping ν_1 $(UO_2)^{2+}$ symmetric stretching vibrations (two uranium atoms in the asymmetric unit of the metarauchite unit-cell), split triply degenerate ν_3 $(AsO_4)^{3-}$ antisymmetric stretching vibration (probably split with regard to factor-group analysis), and n_1 $(AsO_4)^{3-}$ symmetric stretching vibration.

Furthermore, from Figure 10, we infer that a broad band at 818 cm^{-1} in the infrared spectrum has to be attributed to split a triply degenerate ν_3 $(AsO_4)^{3-}$ antisymmetric stretching vibration, because of its high intensity. Consequently, the broad infrared band may comprise overlapping ν_1 $(UO_2)^{2+}$ vibrations as well if they are active. The infrared shoulders located at the higher wavenumbers can be assigned to a component of the ν_3 triply degenerate splitting antisymmetric stretching vibration of the $(AsO_4)^{3-}$ antisymmetric stretching vibration. The infrared band at 947 cm^{-1} is attributed to the ν_3 $(UO_2)^{2+}$ antisymmetric stretching mode. The U–O bond length (~1.8 Å) inferred from this wavenumber (Bartlett & Cooney 1989) is consistent with the value 1.78 Å found for the synthetic analogue (Locock *et al*. 2004).

The doubly degenerate ν_2 $(UO_2)^{2+}$ bending vibration occurs within the region 200–300 cm^{-1} (Čejka 1999). The Raman bands at 248 and 272 cm^{-1} can be assigned

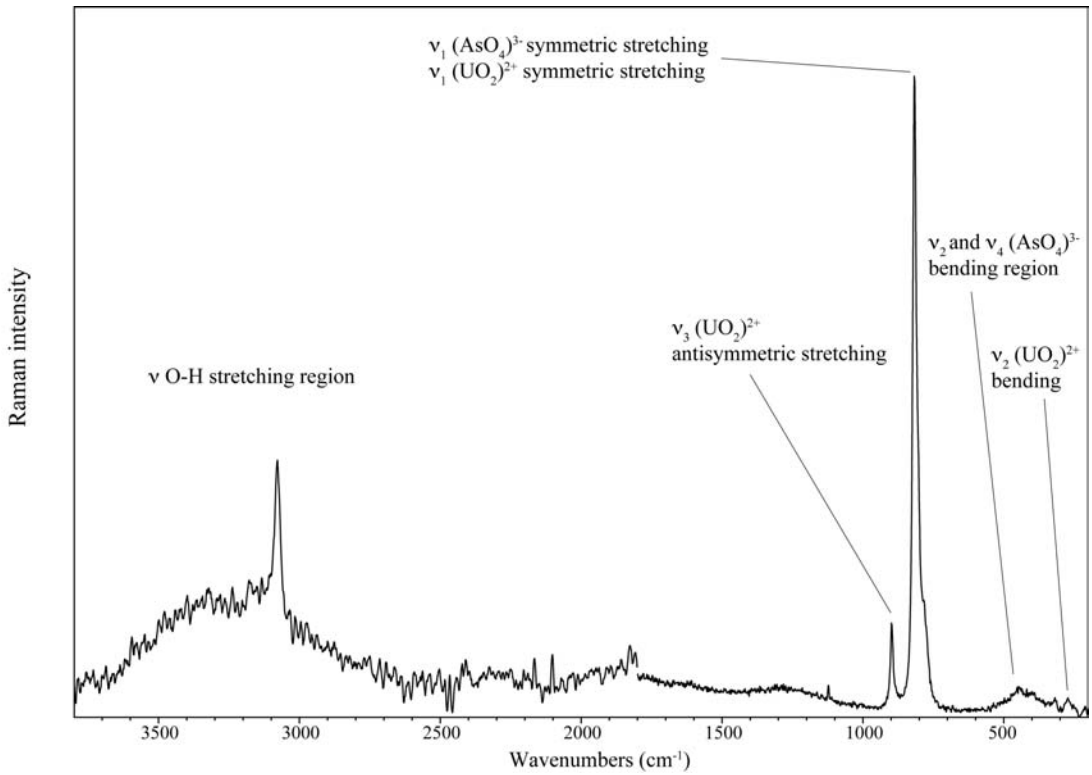

FIG. 8. The Raman spectrum of metarauchite from Jáchymov with tentatively assigned vibration bands. The figure shows two different spectra measured with different accumulation time; the real intensity in the O–H stretching region is much lower than displayed.

to this mode. The relatively intense Raman band at 211 cm^{-1} can be linked to U–PO_4 stretching mode (Čejka & Muck 1984). The (δ) bending modes of $(AsO_4)^{3-}$ tetrahedra, doubly degenerate ν_2 and triply degenerate ν_4 vibrations, are located as broad (split) low-intensity Raman bands at 445, 395, 361 cm^{-1} (ν_4) and 330, 319 cm^{-1} (ν_2).

Presence of $(PO_4)^{3-}$ groups

Vibrations corresponding to stretching vibration modes of $(PO_4)^{3-}$ were not observed in the spectra, with the exception of the absorption in the infrared pattern at 1033 cm^{-1}. This band may be assigned to the antisymmetric stretching modes ν_3 $(PO_4)^{3-}$. The infrared bands located below 660 cm^{-1} may be assigned to the split triply degenerate bending vibration ν_4 (δ) $(PO_4)^{3-}$. The low intensities of these bands can be explained by the small concentrations of $(PO_4)^{3-}$ anions. Signs of the presence of Si–O stretching vibrations indicated by the concentration of Si confirmed by EMPA in both samples of metarauchite are absent.

Metarauchite: Relations to the Autunite Group

Almost all the experimental results suggest that the new mineral, metarauchite, belongs to the

TABLE 6. RAMAN AND INFRARED BANDS OF METARAUCHITE SAMPLE FROM JÁCHYMOV, WITH TENTATIVE ASSIGNMENTS

Raman (cm^{-1})	Infrared (cm^{-1})	Assignment
	3379 s, broad	
3265 w, broad (+)	3259 sh	v OH stretch
3079 mw, sharp (+)	[3539 (+), 3402 (+), 3260 (+), 3201 (+)]	
	1644 mw	δ H_2O bend
	1617 sh	
1124 w, sharp		overtone/combination band or v_3 $(PO_4)^{3-}$ antisymmetric stretching
	1033 w	v_3 $(PO_4)^{3-}$ antisymmetric stretching
911 sh (vw)	947 ms, sh	v_3 $(UO_2)^{2+}$ antisymmetric stretching
	[947 (+), 936 (+)]	
898 ms (+)	893 sh	
893 vw (+)		overlapping band of v_1 $(AsO_4)^{3-}$ symmetric stretching, v_3 $(AsO_4)^{3-}$ antisymmetric stretching and v_1 $(UO_2)^{2+}$ symmetric stretching vibrations
883 vw (+)		
878 vw (+)	818 vs	
817 vs (+)		
804 sh (+)	[899 (+), 869 (+), 844 (+), 818 (+)]	
785 sh (+)		
771 sh (+)		
	737 sh [745 (+)]	libration modes of H_2O
682 vw	663 vw	v_4 $(PO_4)^{3-}$ bending mode
	621 w	
534 vw		v_2 $(PO_4)^{3-}$ bending mode
445 mw (+)		
395 mw (+)		v_4 $(AsO_4)^{3-}$ bending mode
361 w (+)		
330 mw (+)		v_2 $(AsO_4)^{3-}$ bend
319 mw (+)		
248 mw		v_2 (δ) $(UO_7)^{2+}$ bend
272 w		
211 mw		U–PO_4 stretching
204 w		lattice vibrations

(+) bands deduced from decomposition of the spectra. Symbols: vw: very weak, mw: medium weak, w: weak, ms: medium strong, s: strong, vs: very strong, sh: shoulder.

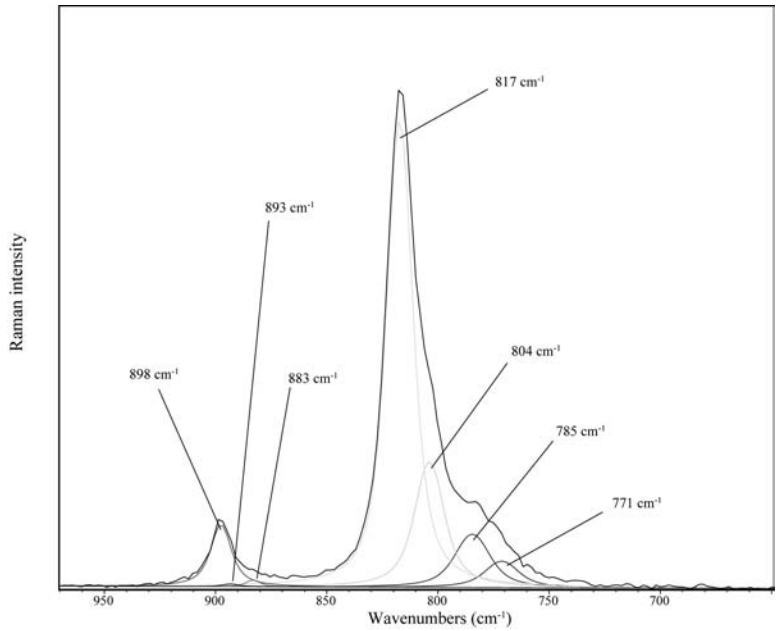

FIG. 9. Decomposition of the Raman spectrum of metarauchite to its band components in the region of overlapping $(AsO_4)^{3-}$ and $(UO_2)^{2+}$ stretching vibrations.

autunite group, characterized by structural sheets of autunite uranyl-anion topology. The interlayer in these compounds can accommodate differently coordinated cations owing to the flexibility of the uranyl tetragonal bipyramids and anion tetrahedra involved in corner sharing in the structural sheets (Locock 2007a). On the basis of the similar ionic radii of Ni and Co (Shannon 1976), we can conclude that metarauchite is isostructural with synthetic metakirchheimerite (Locock *et al*. 2004, Locock 2007a), although single-crystal data for metarauchite are lacking. Furthermore, the Raman spectra indicate that their structures are of the same nature (Fig. 11). Single-crystal studies of the synthetic analogues of hydrated uranyl arsenates and phosphates of divalent metals by Locock *et al*. (2004) show that the symmetry of these minerals is lower, triclinic (in the case of octahydrates), than the tetragonal symmetry believed to pertain earlier. This explains the former problematic assignments of the optical properties (biaxial) of these minerals (*e.g.,* Walenta 1964, Agrinier *et al*. 1972). On the basis of an optical study of metarauchite (optically biaxial) and morphology of its crystals (namely those from Jáchymov), a symmetry lower than tetragonal has to be expected. The Rietveld refinement performed on our sample from Schneeberg is consistent with the hypothesis that metarauchite is triclinic, in view of the low R_{Bragg} indices (Table 2); many reflections in the power pattern of metarauchite cannot be indexed based on the tetragonal unit-cells. Furthermore, the refined unit-cell parameters of metarauchite are consistent with the data reported by Locock *et al*. (2004) for the synthetic analogues.

The broad substitutions observed in the natural samples are possible owing to the similar sizes of the cations. In the case of metarauchite, Mg and Co are mainly involved, leading to the components of metanováčekite and metakirchheimerite. The inference of Locock (2007a) that cations of approximately the same size lead to the same crystal structures is supported by results of the current research.

ACKNOWLEDGEMENTS

We are grateful to Lutz Schlegel, mineral collector from Schneeberg, who discovered and provided the specimens containing metarauchite from the Adam Heber mine. We also thank the Serveis Cientificotècnics of the University of Barcelona for providing the complex analysis (including EMPA, vibration spectroscopy, TGA/DTA and XRD), as well as the expertise that helped us to chracterize the Schneeberg material. Martin Mazuch (Charles University in Prague), Jana Ederová and Vladimír Machovič (Institute of Chemical Technology, Prague) are gratefully acknowledged for their kind help with the measurements. Thanks to Ivan Němec (Charles University in Prague) for his help and

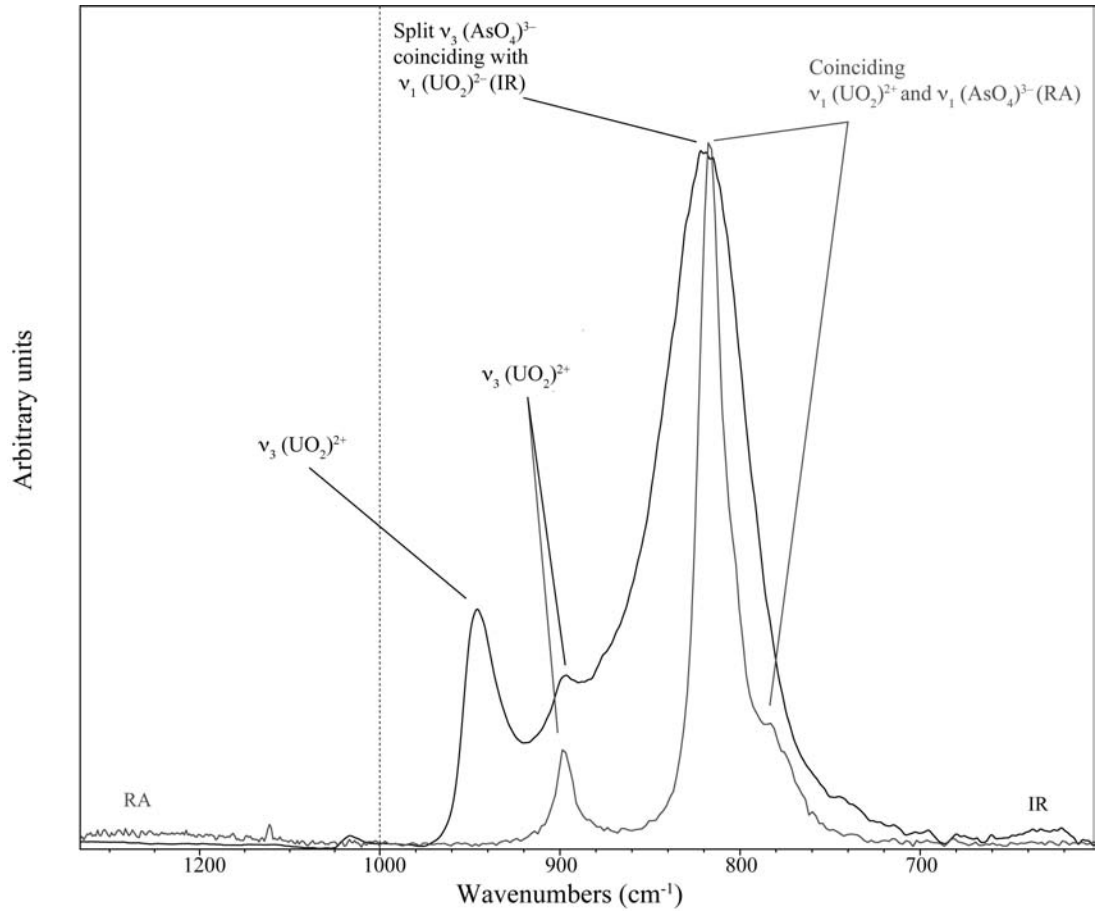

FIG. 10. Comparison of Raman and infrared spectra of metarauchite in the region of overlapping $(AsO_4)^{3-}$ and $(UO_2)^{2+}$ stretching modes.

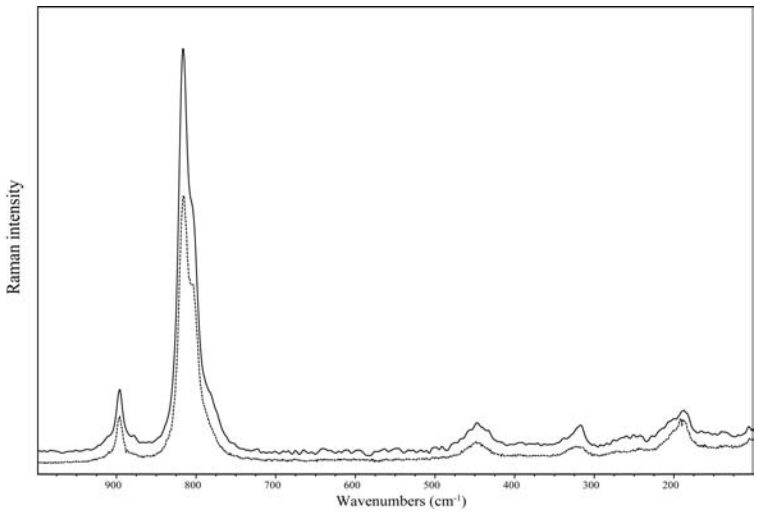

FIG. 11. Comparison of Raman spectra of metarauchite (solid line) and metakirchheimerite (dashed) (Plášil *et al*. 2009) in the region of fundamental $(AsO_4)^{3-}$ and $(UO_2)^{2+}$ vibrations.

valuable comments on infrared spectroscopy. We are grateful to the anonymous referees for their comments and reviews that helped improving the manuscript, and to Robert F. Martin for his careful editorial work. This research was supported by grants from the Grant Agency of the Charles University in Prague (GAUK no. 17008/2008) to JP and of the Ministry of Culture of the Czech Republic (DE07P04OMG003) to JS, from the Ministry of Education of the Czech Republic (MSM0021620855) to VG and the project MSM0021622412 (INCHEMBIOL) to MN, to whom we are very grateful.

References

Agrinier, H., Chantret, F., Geffroy, J., Héry, B., Bachet, B. & Vachey, H. (1972): Une nouvelle espèce minérale: la méta-lodèvite (arséniate hydraté d'uranium et de zinc). *Bull. Soc. fr. Minéral. Cristallogr.* **95**, 360-364.

Bartlett, J.R. & Cooney, R.P. (1989): On the determination of uranium–oxygen bond lengths in dioxouranium(VI) compounds by Raman spectroscopy. *J. Mol. Struct.* **193**, 295-300.

Čejka, J. (1999): Infrared spectra and thermal analysis of the uranyl minerals. *In* Uranium: Mineralogy, Geochemistry and the Environment (P.C. Burns & R. Finch, eds.). *Rev. Mineral.* **38**, 521-622.

Čejka, J. & Muck, A. (1984): To the infrared spectroscopy of natural uranyl phosphates. *Phys. Chem. Minerals* **11**, 172-177.

Cheary, R.W. & Coelho, A.A. (1996): Programs XFIT and FOURYA, deposited in CCP14 Powder Diffraction Library, Engineering and Physical Sciences Research Council, Daresbury Laboratory, Warrington, England, U.K. (http://www.ccp14.ac.uk/tutorial/xfit-95/xfit.htm).

Chernorukov, N.G., Suleimanov, E.V. & Dzhabarova, S.T. (1998): Synthesis and study of compounds formed in the systems $Ni(PUO_6)_2$–H_2O and $Ni(AsUO_6)$–H_2O. *Zh. Neorg. Khim.* **43**, 997-1002 (in Russian).

Chernorukov, N.G., Suleimanov, E.V., Dzhabarova, S.T. & Barch, S.V. (2000): Synthesis and study of compounds of the series $A^{II}(B^{V}UO_6)_2 \bullet nH_2O$ (A^{II} – Mn, Fe, Co, Ni, Cu, Zn; B^{V} – P, As). *Radiochem.* **42**, 15-32.

Gröbner, J. & Kolitsch, U. (2005): Neufunde aus dem Revier Schneeberg im Erzgebirge. *Lapis* **30**(7-8), 71-73.

Herrmann, S. (2005): Geologie, Erzgänge und Mineralisation der Lagerstätte Schneeberg/Sachen. *Lapis* **30**(7-8), 30-40.

Lahl, B. (2005): Von 1470 bis 1956: der Schneeberg Bergau. *Lapis* **30**(7-8), 13-21.

Libowitzky, E. (1999): Correlation of O–H stretching frequencies and O–H...O hydrogen bond lengths in minerals. *Monatsh. Chem.* **130**, 1047-1059.

Locock, A.J. (2004): *Crystal Chemistry of Uranyl Phosphates, Arsenates and Oxysalts of Chromium(V): Implications for Remediation*. Ph.D. thesis, University of Notre Dame, Notre Dame, Indiana.

Locock, A.J. (2007a): Trends in actinide compounds with the autunite sheet-anion topology. *Zap. Vser. Mineral. Obshchest.* **136**(7), 115-137.

Locock, A.J. (2007b): Crystal chemistry of actinide phosphates and arsenates. *In* Structural Chemistry of Inorganic Actinide Compounds (S.V. Krivovichev, P.C. Burns & I. G. Tananaev, eds.). Elsevier, New York, N.Y. (217-278).

Locock, A.J. & Burns, P.C. (2003): Crystal structures and synthesis of the copper-dominant members of the autunite and meta-autunite groups: torbernite, zeunerite, metatorbernite and metazeunerite. *Can. Mineral.* **41**, 489-502.

Locock, A.J., Burns, P.C. & Flynn, T.M. (2004): Divalent transition metals and magnesium in structures that contain the autunite type sheet. *Can. Mineral.* **42**, 1699-1718.

Massanek, A. & Michalski, S. (2005): Die Mineralien des Schneeberg Reviers. *Lapis* **30**(7-8), 41-66.

Nabar, M.A. & Iyer, V.J. (1977): Preparation and crystallographic characterization of uranyl double arsenates $M^{II}(UO_2AsO_4)_2.8H_2O$ (M = Zn, Ni and Co). *Bull Soc. fr. Minéral. Cristallogr.* **100**, 272-274.

Ondruš, P., Skála, R., Císařová, I., Veselovský, F., Frýda, J. & Čejka, J. (2002): Description and crystal structure of vajdakite, $[(Mo^{+6}O_2)_2(H_2O)_2As^{3+}{}_2O_5]\bullet H_2O$ – a new mineral from Jáchymov, Czech Republic. *Am. Mineral.* **87**, 983-990.

Ondruš, P., Veselovský, F., Gabašová, A., Drábek, M., Dobeš, P., Malý, K., Hloušek, J. & Sejkora, J. (2003d): Ore-forming processes and mineral parageneses of the Jáchymov ore district. *J. Czech Geol. Soc.* **48**(3-4), 157-192.

Ondruš, P., Veselovský, F., Gabašová, A., Hloušek, J. & Šrein, V. (2003a): Geology and hydrothermal vein system of the Jáchymov (Joachimsthal) ore district. *J. Czech Geol. Soc.* **48**(3-4), 3-18.

Ondruš, P., Veselovský, F., Gabašová, A., Hloušek, J. & Šrein, V. (2003c): Supplement to secondary and rock-forming minerals of the Jáchymov ore district. *J. Czech Geol. Soc.* **48**(3-4), 149-155.

Ondruš, P., Veselovský, F., Gabašová, A., Hloušek, J., Šrein, V., Vavřín, I., Skála, R., Sejkora, J. & Drábek, M. (2003b): Primary minerals of the Jáchymov ore district. *J. Czech Geol. Soc.* **48**(3-4), 19-147.

Ondruš, P., Veselovský, F., Hloušek, J., Skála, R., Vavřín, I., Frýda, J., Čejka, J. & Gabašová, A. (1997b): Secondary minerals of the Jáchymov (Joachimsthal). *J. Czech Geol. Soc.* **42**, 3-76.

ONDRUŠ, P., VESELOVSKÝ, F., SKÁLA, R., CÍSAŘOVÁ, I., HLOUŠEK, J., FRÝDA, J., VAVŘÍN, I., ČEJKA, J. & GABAŠOVÁ, A. (1997a): New naturally occurring phases of secondary origin from Jáchymov (Joachimsthal). *J. Czech Geol. Soc.* **42**, 77-107.

PLÁŠIL, J. (2009): *Crystal Chemistry of Selected Natural Hydrated Uranylarsenates and Phosphates of Divalent Transition Metals and Magnesium*. M.Sc. thesis, Faculty of Science, Charles University, Prague, Czech Republic.

PLÁŠIL, J., ČEJKA, J., SEJKORA, J., HLOUŠEK, J. & GOLIÁŠ, V. (2009): New data for metakirchheimerite from Jáchymov (St. Joachimsthal), Czech Republic. *J. Geosci.* **54**, 373-384.

PLÁŠIL, J., SEJKORA, J., ČEJKA, J., ŠKÁCHA, P., GOLIÁŠ, V. & EDEROVÁ, J. (2010): Characterization of phosphate-rich metalodèvite from Příbram, Czech Republic. *Can. Mineral.* **48**, 113-122.

POUCHOU, J.L. & PICHOIR, F. (1985): "PAP" $\phi(\rho Z)$ procedure for improved quantitative microanalysis. *In* Microbeam Analysis (J.T. Armstrong, ed.). San Francisco Press, San Francisco, California (104-106).

SABINE, T.M., HUNTER, B.A., SABINE, W.R. & BALL, C.J. (1998): Analytical expressions for the transmission factor and peak shift in absorbing cylindrical specimens. *J. Appl. Crystallogr.* **31**, 47-51.

SHANNON, R.D. (1976): Revised effective ionic radii and systematic studies of interatomic distances in halides and chalcogenides. *Acta Crystallogr.* **A32**, 751-767.

THALHEIM, K. (2005): Der Schneeberg Silverfund von 1477. *Lapis* **30**(7-8), 24-29.

VOCHTEN, R. & GOEMINNE, A. (1984): Synthesis, crystallographic data, solubility and electrokinetic properties of meta-zeunerite, meta-kircheimerite and nickel–uranylarsenate. *Phys. Chem. Minerals* **11**, 95-100.

WALENTA, K. (1964): Beiträge zur Kenntnis seltener Arsenatmineralien unter besonderer Berücksichtigung von Vorkommen des Scharzwaldes. *Tschermaks Miner. Petrogr. Mitt.* **9**, 111-174.

WEISS, S. (2005): Von Brendelit bis Schlegelit: Schneeberg Erstbeschreibungen 1998–2003. *Lapis* **30**(7-8), 67-70.

YOUNG, R.A. (1993): Introduction to the Rietveld method. *In* The Rietveld Method (R.A. Young, ed.). IUCr Book Series, Oxford University Press, Oxford, U.K. (1-39).

Received October 8, 2009, revised manuscript accepted April 5, 2010.